

NUMERICAL DISCRETIZATIONS FOR SHALLOW WATER EQUATIONS WITH SOURCE TERMS ON UNSTRUCTURED MESHES

ARNAUD DURAN AND FABIEN MARCHE

Institut de Mathématiques et de Modélisation de Montpellier (I3M)
Université Montpellier 2, CC 051, 34090 Montpellier, France

CHRISTOPHE BERTHON AND RODOLPHE TURPAULT

Laboratoire de Mathématiques Jean Leray
Université de Nantes, France

ABSTRACT. In the following lines we introduce two frictional schemes for the discretization of the 2D Shallow Water system, on unstructured meshes. The starting point consists in writing both of them as convex combinations of 1D schemes. Then, we propose to include the resistance effects proceeding to a slight adaptation of the gathered convex components, using the frictional approach recently developed in [2]. This method turns out to provide an excellent behavior for vanishing water heights, and does not require a modification of the CFL. Numerical experiments will be performed in order to assess the capacity of the two schemes in dealing with wetting and drying, complex geometry and topography.

Introduction. In this work we consider discretizations of the 2D Non linear Shallow Water equations (NSW). As the name suggests, the NSW model consists in an hyperbolic set of non linear equations, and is used to describe the motion of shallow flows, as flood waves, flooding and drying, dam breaks, or more generally any kind of hydrodynamic processes near coasts or in bed rivers. Denoting h the water height, $\mathbf{q} = {}^t(q_x, q_y)$ the discharge and z a parametrization of the bed slope, we write the set of NSW equations under its conservative form :

$$w_t + \nabla \cdot \mathcal{H}(w) = -\mathcal{B}(w, z) - \mathcal{F}(w), \quad (1)$$

with

$$w = \begin{pmatrix} h \\ q_x \\ q_y \end{pmatrix} \quad \mathcal{H}(w) = \begin{pmatrix} q_x & q_y \\ \frac{q_x^2}{h} + \frac{1}{2}gh^2 & \frac{q_x q_y}{h} \\ \frac{q_x q_y}{h} & \frac{q_y^2}{h} + \frac{1}{2}gh^2 \end{pmatrix}, \quad (2)$$

and the following expressions for bathymetry and friction :

$$\mathcal{B}(w, z) = \begin{pmatrix} 0 \\ ghz_x \\ ghz_y \end{pmatrix} \quad \mathcal{F}(w) = \begin{pmatrix} 0 \\ \kappa \frac{\|q\|}{h^\gamma} q_x \\ \kappa \frac{\|q\|}{h^\gamma} q_y \end{pmatrix}. \quad (3)$$

2000 *Mathematics Subject Classification.* Primary: 58F15, 58F17; Secondary: 53C35.

Key words and phrases. Nonlinear Shallow Water, Finite Volume, Well Balanced schemes, friction, unstructured mesh.

The behavior of the resistance \mathcal{F} is partly governed by the positive constants κ and γ , and may be watched closely as the water elevation tends to zero. A suitable construction of a numerical scheme for the discretization of the Shallow Water system is generally subject to some numerical requirements, discussed in the major part of the published studies on the theme. The first obligation is the well known *well balancing* property, that is the preservation of the following motionless steady state : $\eta = cte$ and $\mathbf{u} = 0$. The second unavoidable property we want to achieve is the robustness, namely the ability to preserve the convex set of admissible states $\Omega = \{(h, q_x, q_y), h \geq 0\}$. Finally, we direct our discussion on the capacity in handling dry cells or low values of the water height, which turns out to be a major concern when the physical model deals with a friction term under the form (3). One of the main objectives of this work consists in proposing numerical schemes offering a stable and accurate treatment of such configurations.

The paper is split up in four parts : in Sections 1 and 2 we propose a detailed presentation of the first scheme, called *BF-scheme* in the sequel. Then, we briefly give some words regarding a second order extension, and discuss about a twin numerical approach. The last part is devoted to numerical tests expected to validate and compare the abilities of the two schemes resulting from these developments.

1. Frictionless scheme. The following approach has been developed by Berthon, first in a 1D framework, leading to a well balanced and robust scheme, with an excellent behavior in the neighborhood of dry cells. Before caring about the inclusion of friction, we propose to set up the main results and notations related to its extension in the context of unstructured triangulations (see also [3]).

The choice of $W = {}^t(\eta, \eta u, \eta v)$ instead of w as conservative vector variable during the evaluation of the numerical fluxes leads to the following alternative form of homogeneous NSW :

$$w_t + \nabla \cdot \left(\xi \mathcal{H}(W) - \begin{pmatrix} 0 & 0 \\ \frac{ghz}{2} & 0 \\ 0 & \frac{ghz}{2} \end{pmatrix} \right) = 0, \quad (4)$$

where we introduced the new variable $\xi = h/\eta$. In this first part we seek a discretization of (4) in an unstructured context. To this purpose, let's introduce some notations concerning the geometry : we consider the dual mesh related to a triangulation \mathcal{T} of the computational domain. The nodes of \mathcal{T} will be denoted $(S_i)_i$, the elements $(T_i)_i$, and the vertex centered cells $(C_i)_i$. In what follows, K_i will refer to the set of subscripts j for which C_j is adjacent to C_i , and l_{ij} the length of the associated interface Γ_{ij} ; a basic example of geometry is available on Fig. 1, where other useful notations are given. Denoting $w_i^n = (h_i^n, q_{x,i}^n, q_{y,i}^n)$ a constant interpolation of the solution at the cell C_i at time t^n , we chose to evolve this approximate state gathering the components of a 3 points 1D scheme (Fig. 1 - 2) :

$$w_i^{n+1} = \sum_{j \in K_i} \frac{|T_{ij}|}{C_i} \tilde{w}_{ij}^{n+1}, \quad (5)$$

$$\tilde{w}_{ij}^{n+1} = w_i^n - \frac{\Delta t}{|T_{ij}|} l_{ij} (\phi(w_i^n, w_j^n, \vec{n}_{ij}) - \phi(w_i^n, w_i^n, \vec{n}_{ij})). \quad (6)$$

Herein, referring to [3], the numerical fluxes ϕ are defined by :

$$\phi(w_i^n, w_j^n, \vec{n}_{ij}) = X_{ij} H(W_i^n, W_j^n, \vec{n}_{ij}), \quad (7)$$

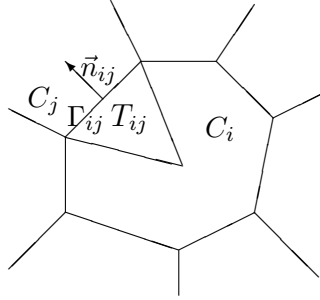
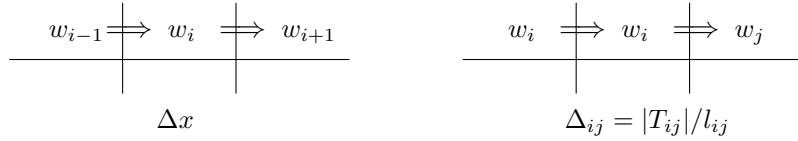
FIGURE 1. Dual cell C_i issuing from \mathcal{T} ; notations at the interface Γ_{ij} .

FIGURE 2. Left and right Riemann states for the 1D and 2D schemes.

where $H = H(U, V, \vec{n})$ denotes a flux function for $\mathcal{H} \cdot \vec{n}$, and :

$$X_{ij} = \begin{cases} \xi_i^n & \text{if } H^h(W_i^n, W_j^n, \vec{n}_{ij}) \geq 0, \\ \xi_j^n & \text{otherwise.} \end{cases} \quad (8)$$

Remark 1. In what follows, the function $H : (U, V, \vec{n}) \mapsto H(U, V, \vec{n})$ would be supposed to verify these two classical properties :

$$\text{consistency : } H(W, W, \vec{n}) = \mathcal{H}(W) \cdot \vec{n} \quad \forall W \in \Omega. \quad (9)$$

$$\text{conservativity : } H(U, V, \vec{n}) = -H(V, U, -\vec{n}) \quad \forall U, V \in \Omega. \quad (10)$$

From a practical point of view, computations will be performed using the HLLC or VFRoe - relaxation solver, which associated fluxes are known to fulfill the numerical requirements mentioned above, and handling with contact discontinuities.

Hence, according to (10), the “left” fluxes in (6) just reads : $\phi(w_i^n, w_i^n, \vec{n}_{ij}) = \frac{h_i^n}{\eta_i^n}(\mathcal{H}(w_i^n) \cdot \vec{n}_{ij})$, and calling Green’s formula, we obtain :

$$w_i^{n+1} = w_i^n - \frac{\Delta t}{|C_i|} \sum_{j \in K_i} l_{ij} \phi(w_i^n, w_j^n, \vec{n}_{ij}). \quad (11)$$

We finally complete this discretization of NSW considering the treatment of the bathymetry $\mathcal{B}(w, z)$. In accordance with [3], we denote :

$$H_{ij} = \begin{cases} \eta_i^n & \text{if } H^h(W_i^n, W_j^n, \vec{n}_{ij}) \geq 0, \\ \eta_j^n & \text{otherwise.} \end{cases}, \quad (12)$$

and chose the following discretization for the bed slope source term :

$$B_{ij} = \frac{g}{2} \begin{pmatrix} 0 \\ H_{ij} \eta_i^n (X_{ij} - \xi_i^n) \vec{n}_{ij} \end{pmatrix}, \quad (13)$$

to write :

$$w_i^{n+1} = w_i^n - \frac{\Delta t}{|C_i|} \sum_{j \in K_i} l_{ij} (\phi(w_i^n, w_j^n, \vec{n}_{ij}) - B_{ij}). \quad (14)$$

We emphasize that the resulting scheme has been shown to be well balanced and robust under the following CFL condition :

$$\Delta t \max_{i \in \mathbb{Z}, j \in K_i} \frac{l_{ij}}{|T_{ij}|} |\lambda_{ij}^\pm| < \frac{1}{2}, \quad (15)$$

supplemented by the following CFL restriction :

$$\Delta t \max_{i \in \mathbb{Z}, j \in K_i} \left[\frac{l_{ij}}{|T_{ij}|} \left(\max(0, H^h(W_i, W_j, \vec{n}_{ij})) - \min(0, \mathcal{H}^h(W_i) \cdot \vec{n}_{ij}) \right) \right] < \eta_i^n, \quad (16)$$

where the velocity waves λ_{ij}^\pm in (15) refers to the upper and lower extremities of the Riemann solver's dependancy cone. Actually, the proofs are straightforward, getting back to the formulation (5,6) and invoking the properties of the 1D approach.

2. Friction scheme. As shown in [2], in a 1D context, we can achieve a robust numerical treatment of the resistance terms considering a suitable adaptation of the Riemann states involved in the fluxes. More precisely, the proposed scheme is based on the use of the following modified HLL Riemann solver :

$$\tilde{w}_R\left(\frac{x}{t}, w_L, w_R\right) = \begin{cases} w_L \text{ if } \frac{x}{t} \leq a^- \\ w^* + (1-\alpha)(w_L^* - w^* - \frac{h^\gamma}{\kappa} \mathcal{F}(w_L)) \text{ if } a^- \leq \frac{x}{t} \leq 0 \\ w^* + (1-\alpha)(w_R^* - w^* - \frac{h^\gamma}{\kappa} \mathcal{F}(w_R)) \text{ if } 0 \leq \frac{x}{t} \leq a^+ \\ w_R \text{ if } \frac{x}{t} \geq a^+ \end{cases}, \quad (17)$$

where w^* stands for the HLL intermediate state :

$$w^*\left(\frac{x}{t}, w_L, w_R\right) = \frac{a^+ w_R - a^- w_L}{a^+ - a^-} (\mathcal{H}(w_R) - \mathcal{H}(w_L)), \text{ and} \quad (18)$$

$$w_L\left(\frac{x}{t}, w_L, w_R\right) = \left(\frac{h^*\left(\frac{x}{t}, w_L, w_R\right)}{(hu)_L} \right), \quad w_R\left(\frac{x}{t}, w_L, w_R\right) = \left(\frac{h^*\left(\frac{x}{t}, w_L, w_R\right)}{(hu)_R} \right). \quad (19)$$

Herein, \mathcal{H} denotes the monodimensional exact flux function of the NSW equations, and a^\pm are the maximum and minimum velocity waves involved in the Riemann solver. Obviously, there is a close dependance between the leading friction parameter α and the friction source term $\mathcal{F}(w)$. A discretization will be proposed later on, covering Darcy and Manning friction laws (see Section 4). Actually, such choice is also submitted to some specific requirements, and we refer to [2] for more details. In a 1D context, using consistency relations and an appropriate analysis of the wave speeds involved in the HLL solver, we obtain the following scheme :

$$\begin{aligned} h_i^{n+1} &= h_i^n - \frac{\Delta t}{\Delta x} (H_{i+\frac{1}{2}}^h - H_{i-\frac{1}{2}}^h), \\ (hu)_i^{n+1} &= (hu)_i^n - \frac{\Delta t}{\Delta x} \left[\alpha_{i+\frac{1}{2}} H_{i+\frac{1}{2}}^{hu} - \alpha_{i-\frac{1}{2}} H_{i-\frac{1}{2}}^{hu} - \right. \\ &\quad \left. ((1 - \alpha_{i-\frac{1}{2}}) s_{i-\frac{1}{2}}^{+,hu} + (1 - \alpha_{i+\frac{1}{2}}) s_{i+\frac{1}{2}}^{-,hu}) \right], \end{aligned} \quad (20)$$

where $H_{i+\frac{1}{2}}$ stands for an interpolation of $\mathcal{H}(w)$ at the node $i + 1/2$. The friction terms are defined by :

- $\alpha_{i+1/2} = \frac{(a_{i+1/2}^+ - a_{i+1/2}^-)}{(a_{i+1/2}^+ - a_{i+1/2}^-) + \mathcal{F}_{i+1/2} \Delta x}$.
- $\mathcal{F}_{i+1/2} = \frac{\kappa q_{i+1/2}}{h_{i+1/2}}, h_{i+1/2} = \frac{(h_i^n)^\gamma + (h_{i+1}^n)^\gamma}{2}, q_{i+1/2} = \frac{\|\mathbf{q}_i^n\| + \|\mathbf{q}_{i+1}^n\|}{2}$.
- $s_{i+1/2}^{-,hu} = \min(0, a_{i+1/2}^-) (hu)_i^n - \min(0, a_{i+1/2}^+) (hu)_{i+1}^n - \mathcal{H}^{hu}(w_i^n)$.

$$\bullet \quad s_{i-1/2}^{+,hu} = \max(0, a_{i-1/2}^-(hu))_{i-1} - \max(0, a_{i-1/2}^+(hu))_i + \mathcal{H}^{hu}(w_i^n).$$

Remark 2. In the pioneer paper, the evaluation of the numerical fluxes $H_{i+1/2}$ is performed with the HLL relaxation solver. In practise, computations with any other consistent and conservative flux function in the (1D) sense of (9) and (10) (as those provided by the HLLC and VF Roe solver) remains valid.

Now, in order to perform an extension to the unstructured case, we chose to extrapolate formulas (20), defining the convex components as :

$$\begin{aligned} \tilde{h}_{ij}^n &= h_i^n - \frac{\Delta t}{\Delta_{ij}} (\phi^h(w_i^n, w_j^n, \vec{n}_{ij}) - \phi^h(w_i^n, w_i^n, \vec{n}_{ij})) , \\ (\tilde{hu})_{ij}^n &= (hu)_i^n - \frac{\Delta t}{\Delta_{ij}} \left[\alpha_{ij}\phi^{hu}(w_i^n, w_j^n, \vec{n}_{ij}) - \alpha_{ii}\phi^{hu}(w_i^n, w_i^n, \vec{n}_{ij}) \right. \\ &\quad \left. - \left((1 - \alpha_{ii})s_{ii}^{+,hu} + (1 - \alpha_{ij})s_{ij}^{-,hu} \right) \right] , \\ (\tilde{hv})_{ij}^n &= (hv)_i^n - \frac{\Delta t}{\Delta_{ij}} \left[\alpha_{ij}\phi^{hv}(w_i^n, w_j^n, \vec{n}_{ij}) - \alpha_{ii}\phi^{hv}(w_i^n, w_i^n, \vec{n}_{ij}) \right. \\ &\quad \left. - \left((1 - \alpha_{ii})s_{ii}^{+,hv} + (1 - \alpha_{ij})s_{ij}^{-,hv} \right) \right] . \end{aligned} \quad (21)$$

These 1D updates are then gathered using (5) ; introducing the terms (13) related to the topography, we obtain the following scheme :

$$\begin{aligned} h_i^{n+1} &= h_i^n - \frac{\Delta t}{|C_i|} \sum_{j \in K_i} l_{ij} \Delta \phi_{ij}^h , \\ (hu)_i^{n+1} &= (hu)_i^n - \frac{\Delta t}{|C_i|} \sum_{j \in K_i} l_{ij} (\Delta \phi_{ij}^{hu} - \Delta s_{ij}^{hu} - B_{ij}^{hu}) , \\ (hv)_i^{n+1} &= (hv)_i^n - \frac{\Delta t}{|C_i|} \sum_{j \in K_i} l_{ij} (\Delta \phi_{ij}^{hv} - \Delta s_{ij}^{hv} - B_{ij}^{hv}) , \end{aligned} \quad (22)$$

with

$$\Delta \phi_{ij} = \begin{pmatrix} \phi^h(w_i^n, w_j^n, \vec{n}_{ij}) - \phi^h(w_i^n, w_i^n, \vec{n}_{ij}) \\ \alpha_{ij}\phi^{hu}(w_i^n, w_j^n, \vec{n}_{ij}) - \alpha_{ii}\phi^{hu}(w_i^n, w_i^n, \vec{n}_{ij}) \\ \alpha_{ij}\phi^{hv}(w_i^n, w_j^n, \vec{n}_{ij}) - \alpha_{ii}\phi^{hv}(w_i^n, w_i^n, \vec{n}_{ij}) \end{pmatrix} , \quad (23)$$

and

$$\Delta s_{ij} = \begin{pmatrix} (1 - \alpha_{ii})s_{ii}^{+,hu} + (1 - \alpha_{ij})s_{ij}^{-,hu} \\ (1 - \alpha_{ii})s_{ii}^{+,hv} + (1 - \alpha_{ij})s_{ij}^{-,hv} \end{pmatrix} . \quad (24)$$

Remark 3. When $\kappa = 0$, the leading friction parameter α_{ij} is obviously equal to 1, and we recover the condensed formulation established in the frictionless case (14).

Remark 4. One of the main features of the current frictional scheme is that we do not have to use a more restrictive CFL to ensure the robustness property. Indeed, we can easily verify that formulas (22-23) and (14) are equivalent for the water height.

3. Additional investigations. We first discuss about a second order extension of the BF-scheme (22-24). In order to improve the accuracy, we chose to adopt the reconstruction technique introduced in [4], following closely the lines of [7]. Avoiding redundancies, we do not give details on this method here, and just propose a brief overview of the final results. Actually, we simply reach an analogous formulation of (22-24), where the original values have been replaced by the second order ones. After straightforward computations, the proof of the well balancing property appears to be the same as in the first order case, and the preservation of the water height positivity is ensured provided a slight adaptation of the additional CFL restriction (16), involving the second order values W_{ij} and W_{ji} :

$$\Delta t \max_{i \in \mathbb{Z}, j \in K_i} \left[\frac{l_{ij}}{|T_{ij}|} \left(\max(0, H^h(W_{ij}, W_{ij}, \vec{n}_{ij})) - \min(0, \mathcal{H}^h(W_i) \cdot \vec{n}_{ij}) \right) \right] < \eta_i^n . \quad (25)$$

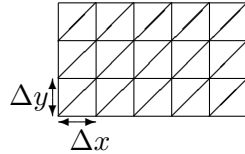


FIGURE 3. Triangulation issuing from a cartesian mesh.

In a second hand, we point out that the main strategy of this work consists in the creation of a 2D discretization of NSW using a 3 point monodimensional scheme (formulation 5 - 6). In reality, this technique is not restricted to the only use of Berthon's scheme, and can also be run considering another 1D approach. Indeed, we mention that the lines of Sections 1 and 2 can be followed taking the 1D *pre balanced* scheme developed by Liang *et al.* in [9] as starting point. Considering the similarities with the two previous sections, we neither go further in the developments. We just note that the resulting scheme is very close than the one described in [7] for the frictionless case, with the advantage of ensuring the preservation of the admissible states under a less restrictive CFL. As for the BF case, the inclusion of the resistance and the second order extension previously discussed can also be performed, preserving the well balancing property ; however we refer to [7] for the proof of the robustness at order 2, which requires additional work. We mention that deeper investigations are currently in progress on the subject [8] ; the scheme obtained in this way will be called the *LF-scheme* in the next section.

4. Numerical Validations.

4.1. Dam break with friction. We consider a classical one - dimensional dam break problem with friction on a flat bottom. One can build an approximation of the exact solution by splitting the domain in two regions behind the wave front location ; in the first area, frictional effects can be neglected ; the exact solution is provided considering an ideal fluid flow model for Shallow Water equations. In the wave tip region bed, the variation of the wave speed is small, and the resistance phenomena becomes dominant under acceleration and inertia effects. Physical and mathematical issues of such construction are detailed in [6]. In a 2D framework, we will consider a rectangular channel with dimensions $[-10, 10] \times [0, 4]$. The initial water depth is set to 1m at the left of the dam ($x \leq 0$), and 0 elsewhere. For this test, we consider a Darcy friction law : $\mathcal{F}(w) = (0, (f/8) \|\mathbf{u}\|u, (f/8) \|\mathbf{u}\|v)$, and recover the formulation (3) with $\gamma = 2$ and $\kappa = f/8$. The Darcy coefficient is set to $f = 0.05$, and we use a 8241 nodes splitted cartesian grid, with $\Delta x = \Delta y = 0.1m$ (Fig. 3). Fig. 4 shows some snapshots of the water depth along the middle section, until $t = 2.5s$. We can observe a good agreement with the analytical solution ; the wave front location seems to be accurately computed, which tends to validate the ability of the BF and LF schemes to deal with wetting and drying. We can also point out the good concordance with the predictions provided by the work of Céa *et al* in [5].

4.2. Moving boundary over a parabolic bottom. The following test is also issuing from a 1D benchmark simulation for NSW models (see [9]), derived itself from a test case proposed by Thacker in 1981 (see [10]). Initially, the domain is assumed to be a 8640m length channel, and we set its width to 1000m for a 2D extrapolation. Computations are run on a regular triangulation (Fig. 3) with $\Delta x = 27m$, $\Delta y = 25m$, and the parametrization of the bathymetry is given by:

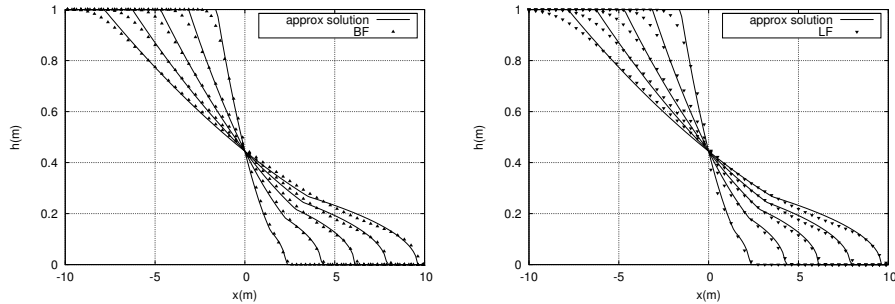


FIGURE 4. Dam break with friction : water depth profiles at $t=0.5$, 1 , 1.5 , 2 and 2.5 s for the BF (left) and LF (right) schemes.

$$z(x, y) = h_0 \left(\left(\frac{x}{a} \right)^2 - 1 \right).$$

This time, we consider a linear friction term : $\mathcal{F}(w) = {}^t(0, \kappa h u, \kappa h v)$. As we do not enter in the formalism (3), the simulation will be run with the following adaptation of the friction parameter (see (20) and below) : $\mathcal{F}_{i+1/2} = \kappa$. This test involves an oscillatory planar flow, which motion is described by the following equations :

$$\begin{aligned} h(t, x, y) &= \frac{a^2 B^2 e^{-\kappa t}}{8g^2 h_0} \left(-s \kappa \sin(2st) + \left(\frac{\kappa^2}{4} - s^2 \right) \cos(2st) \right) \\ &\quad - \frac{B^2 e^{-\kappa t}}{4g} - \frac{e^{-\kappa t/2}}{g} \left(B s \cos(st) + \frac{\kappa B}{2} \sin(st) \right) x, \\ u(t, x, y) &= B e^{-\kappa t/2} \sin(st), \end{aligned} \quad (26)$$

where $s = \sqrt{(8gh_0/a^2 - \kappa^2)/2}$. For the simulation, the governing parameter for the bed friction term is fixed to $\kappa = 0.001$, and we also set $h_0 = 10m$, $a = 3000m$ and $B = 5m/s$. The periodic motion being submitted to non negligible frictional effects, the amplitude of the oscillations is expected to decrease with respect to time, until the apparition of a motionless steady state in the center of the channel. Such phenomena should be highlighted by the time history of the predicted shoreline location, which is compared to the exact one (see Fig. 5) until time $T = 10000s$:

$$x = \frac{a^2 e^{-\kappa t/2}}{2gh_0} \left(-B s \cos(st) - \frac{\kappa B}{2} \sin(st) \right) \pm a. \quad (27)$$

We now discuss about the behavior of the first and second order schemes toward the numerical error. To do so, we chose to gradually increase the refinement of the mesh, taking respectively $\Delta x = 192, 96, 48$ and $24m$ as discretization steps. On Fig. 6 we can see the evolution of the L^1 -error with respect to Δx , in a log-log scale. Concerning the error on the water height (left), we reach a convergence rate of 0.95 for both first order LF and BF schemes, and 1.53 for the second order reconstruction. Similar results are obtained for the normal discharge (right). As in the first test, the two schemes seem to offer similar results in terms of accuracy, although the second order reconstruction seems to be slightly more efficient for the LF-scheme in this case.

4.3. Malpasset Dam Break. We finally validate the capacity of the two approaches in handling with complex geometry and wetting and drying in a real-world 2D case, proceeding to the Malpasset Dam Break benchmark test. This dam was located in the Department of Var, in the south of France, and collapsed in December

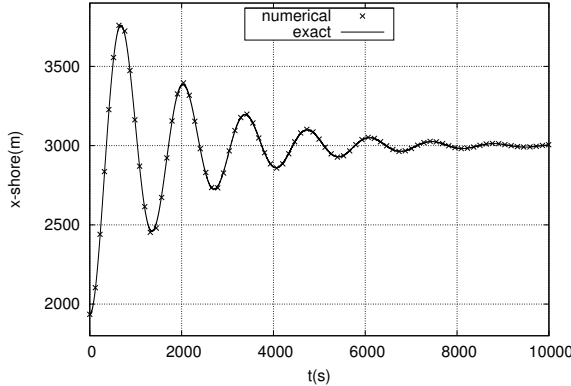


FIGURE 5. Moving boundary over a parabolic bottom : time history of the shoreline location in the right side of the channel. Analytical vs numerical.

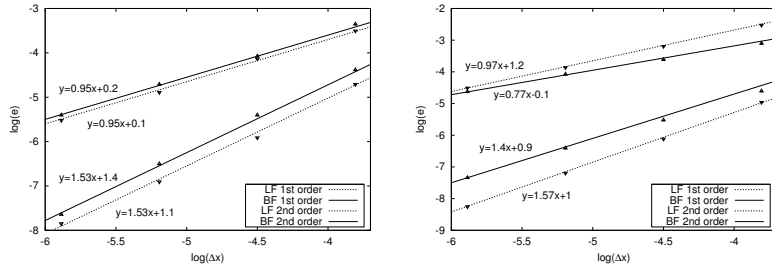


FIGURE 6. Moving boundary over a parabolic bottom : convergence rate analysis for the LF and BF schemes (error computed at $t=370s$).

1959. Thanks to the bathymetric and geometric data available, we run the computations in a vertex centered mesh issuing from a triangulation of 13541 nodes, in which we enforce the value of z . Among the many possibilities for the definition of the bed friction, we chose to consider the Manning-Chezy formulation :

$$\mathcal{F}(w) = \begin{pmatrix} 0 \\ n^2 \frac{\|\mathbf{q}\|}{h^{10/3}} q_x \\ n^2 \frac{\|\mathbf{q}\|}{h^{10/3}} q_y \end{pmatrix}, \quad (28)$$

and set up the Manning coefficient to $n = 0.03$. We follow the time evolution of the location of the flood wave, for which we have a reference at several gauges along the river, provided by a physical experimentation on a reduced model. The predicted arrival time of the water front at gauges 6 to 14 are plotted on Fig. 7, and compared to the reference. Numerical and experimental data only differs from 20s to the maximum : reaching such level of accuracy in this difficult context highlights the real efficiency of the BF and LF schemes.

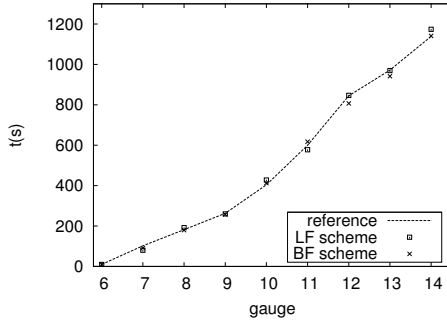


FIGURE 7. Malpasset Dam Break : comparison of predicted wave front propagation time with experimental data at gauges 6 to 14.

REFERENCES

- [1] E. Audusse, F. Bouchut, M.-O. Bristeau, R. Klein, and B. Perthame, *A fast and stable well-balanced scheme with hydrostatic reconstruction for shallow water flows*, SIAM J. Sci. Comput., **25** (6) (2004) : 2050–2065.
- [2] C. Berthon, F. Marche, and R. Turpault, *An efficient scheme on wet/dry transitions for shallow water equations with friction*, Computers and Fluids, **48** (1) (2011) : 192 – 201.
- [3] C. Berthon, F. Foucher, *Efficient well balanced hydrostatic upwind schemes for shallow water equations*, J. Comput. Phys., **231** (15) (2012), 4993–5015.
- [4] S. Camarri, M.V. Salvetti, B. Koobus, and A. Dervieux, *A low-diffusion muscl scheme for les on unstructured grids*, Computers and Fluids, **33** (9) (2004), 1101–1129.
- [5] L. Cea, M.E Vázquez-Cendón, *Unstructured finite volume discretization of bed friction and convective flux in solute transport models linked to the shallow water equations*, J. Comput. Phys. Volume, **231** (8) (2012), 3317–3339.
- [6] H. Chanson, *Analytical solution of dam break wave with flow resistance, Application to tsunami surges*, XXXI Congress, IHAR, (2005), 3341–3353.
- [7] A. Duran, F. Marche, Q. Liang, *On the well-balanced numerical discretization of shallow water equations on unstructured meshes*, J. Comput. Phys., (2012).
- [8] A. Duran, *A robust frictional scheme for the 2D Saint-Venant system on unstructured meshes*, work in progress.
- [9] Q. Liang and F. Marche, *Numerical resolution of well-balanced shallow water equations with complex source terms*, Advances in Water Resources, **32** (6) (2009), 873 – 884.
- [10] W.C. Thacker, *Some exact solutions to the nonlinear shallow water wave equations*, J. Fluid Mech., **107** (1981), 499–508.

E-mail address: Arnaud.Duran@math.univ-montp2.fr